# A Source Term for Wave Attenuation by Sea Ice in WAVEWATCH III®: IC4

CLARENCE O. COLLINS III
W. ERICK ROGERS

*Ocean Dynamics and Prediction Branch*
*Oceanography Division*

June 7, 2017

# REPORT DOCUMENTATION PAGE

| 1. REPORT DATE *(DD-MM-YYYY)* 07-06-2017 | 2. REPORT TYPE Memorandum Report | 3. DATES COVERED *(From - To)* |
|---|---|---|

**4. TITLE AND SUBTITLE**

A Source Term for Wave Attenuation by Sea Ice in WAVEWATCH III®: IC4

**5a. CONTRACT NUMBER**

**5b. GRANT NUMBER**

**5c. PROGRAM ELEMENT NUMBER**

**6. AUTHOR(S)**

Clarence O. Collins III and W. Erick Rogers

**5d. PROJECT NUMBER**

**5e. TASK NUMBER**

**5f. WORK UNIT NUMBER**
73-N2K2-07-5

**7. PERFORMING ORGANIZATION NAME(S) AND ADDRESS(ES)**

Naval Research Laboratory
Oceanography Division
Stennis Space Center, MS 39529-5004

**8. PERFORMING ORGANIZATION REPORT NUMBER**

NRL/MR/7320--17-9726

**9. SPONSORING / MONITORING AGENCY NAME(S) AND ADDRESS(ES)**

Naval Research Laboratory
Director of Research, Code 1001
4555 Overlook Avenue, SW
Washington, DC 20375

**10. SPONSOR / MONITOR'S ACRONYM(S)**

NRL

**11. SPONSOR / MONITOR'S REPORT NUMBER(S)**

**12. DISTRIBUTION / AVAILABILITY STATEMENT**

Approved for public release; distribution is unlimited.

**13. SUPPLEMENTARY NOTES**

**14. ABSTRACT**

This document describes IC4, a new source term for attenuation of wave energy due to the presence of ice. IC4 was developed within the framework of WAVEWATCH III® (WAVEWATCH III® Development Group, 2016). The design criterion for IC4 was a simple, efficient, and flexible implementation of frequency/period dependent wave attenuation. Within IC4, there are 6 methods called M1-M6. M1 to M4 are taken from the literature, though M1, M2, and M4 permit the user to modify the default coefficients. M5 and M6 are input methods for user-defined step functions. Herein, we describe in detail the implementation in the WAVEWATCH III® framework, theoretical and empirical underpinnings of M1-6, give idealized examples, and present a case study based on the data from a field campaign sponsored by the Office of Naval Research. Considering the simplicity of the methods, performance of some IC4 methods in the case study was satisfactory. We demonstrate that frequency dependent attenuation in necessary to replicate the low-pass effect of wave-ice interaction. None of the methods performed universally well under varied ice conditions, which points to the major flaw of a "one size fits all" approach, i.e. attenuation derived from one kind of ice conditions will inevitably fail to reproduce attenuation under conditions which are quite different. We offer IC4 as simple alternative to more complex formulations of wave-ice interaction, but the user is cautioned to understand its limitations.

**15. SUBJECT TERMS**

| | | |
|---|---|---|
| Wave–ice interaction | Ocean surface waves | Spectral wave modeling |
| Wave model | Arctic Ocean | Source terms |
| Sea ice | WAVEWATCH III | Wave hindcasting |

| 16. SECURITY CLASSIFICATION OF: | | | 17. LIMITATION OF ABSTRACT | 18. NUMBER OF PAGES | 19a. NAME OF RESPONSIBLE PERSON W. Erick Rogers |
|---|---|---|---|---|---|
| **a. REPORT** Unclassified Unlimited | **b. ABSTRACT** Unclassified Unlimited | **c. THIS PAGE** Unclassified Unlimited | Unclassified Unlimited | 32 | **19b. TELEPHONE NUMBER** *(include area code)* (228) 688-4727 |

# CONTENTS

# TABLE OF FIGURES

# TABLE OF TABLES

# EXECUTIVE SUMMARY

This document describes IC4, a new source term for attenuation of wave energy due to the presence of ice. IC4 was developed within the framework of WAVEWATCH III® (WAVEWATCH III® Development Group, 2016). The design criterion for IC4 was a simple, efficient, and flexible implementation of frequency/period dependent wave attenuation. Within IC4, there are 6 methods called M1-6. M1 and M2 allow the user control over the shape attenuation function. M1 as an exponential function of wave period and M2 as a $4^{th}$ degree polynomial in wave period. The default coefficients for M1 are based on a fit to the measurements of Wadhams et al. (1988). In M2, the polynomial equation and its default coefficients are based on Meylan et al. (2014). M3 is a fit to theoretical scattering model of Kohout et al. (2008), derived in Horvat and Tziperman (2015), which depends on ice thickness. M4 is based on the work of Kohout et al. (2014), which varies attenuation as a function of significant wave height and is the only method in which attenuation is not a function of frequency. M5 and M6 are two formats for user-defined step functions. Herein, we describe in detail the implementation in the WAVEWATCH III® framework, theoretical and empirical underpinnings of M1-6, give idealized examples, and present a case study based on the data from the field campaign portion of the Office of Naval Research sponsored "Sea State and Boundary Layer Physics in the Emerging Arctic Ocean". Considering the simplicity of the methods, performance of some IC4 methods in the case study was reasonable; particularly so for IC4M6, which is unsurprising, since its functional form was inverted from a sub-set of the Sea State data. IC4M4, while having some skill for total energy, exhibited poor bias in $m_4$, a metric sensitive to energy in the high frequency face of the spectrum, which highlights the fact that frequency dependent attenuation in necessary to replicate the low-pass effect of wave-ice interaction. Even with IC4M6, none of the methods performed universally well under varied ice conditions, which points to the major flaw of a "one size fits all" approach, i.e. attenuation derived from one kind of ice conditions will inevitably fail to reproduce attenuation under conditions which are quite different. Thus, we offer IC4 as simple alternative to more complex formulations of wave-ice interaction, but the user is cautioned to understand its limitations.

# 1 Introduction

The wave environment in the Arctic is changing, as documented in Thomson and Rogers, (2014) and others, and there is an impetus to improve wave prediction in icy waters. Improved prediction requires better understanding of all aspects of wave-ice interaction, reviews of which are taken up in Wadhams et al., (2000), Squire et al., (2007) and Collins et al., (2016a), including attenuation (Squire and Moore, 1980; Wadhams et al., 1988), dispersion (Mosig et al., 2015, Collins et al., 2016b), and ice response including break up events (Asplin et al., 2012; Asplin et al., 2014; Kohout et al., 2014; Collins et al., 2015). This report focuses on phenomenon of attenuation.

As of the Oct. 30th, 2016 release of 3G spectral wave model WAVEWATCH III[®] v5.16 (WW3) (WAVEWATCH III[®] Development Group, 2016) there are 4 available source terms, $S_{ice}$, that act as a sink of wave energy. The first three routines are referred to as IC1, IC2, and IC3 (Rogers and Orzech, 2013; Rogers and Zieger, 2014a, b). Here we introduce and document a fourth routine, IC4. IC4 gives the option to implement one of several simple, empirical attenuation schemes for highly parameterized wave-ice interaction physics.

The motivation for IC4 was to provide a very simple, flexible, and efficient source term that reproduces, albeit through unsophisticated parameterization, some basic know features of wave-ice interaction. IC4, like IC1, only results in attenuation and does not consider dispersion in general, thus shoaling and refraction are unaccounted for.

Within IC4, there are of 6 methods (shorthand M#) for given for applying attenuation. M1-3, M5, and M6 are frequency-dependent, whereas the M4, like IC1, attenuation is uniform across the frequencies. In contrast to IC1, attenuation in M4 varies depending on the wave height. Each method offers a different flavor of attenuation: M1) an exponential fit to the field data of Wadhams et al. (1988); M2) the polynomial fit in Meylan et al. (2014); M3) a quadratic fit to the calculations of Kohout and Meylan (2008) given in Horvat and Tziperman (2015); M4) Eq. 1 of Kohout et al. (2014); M5) a four part step function in frequency space; M6) and an expanded version of M5 with up to 10 steps.

The remainder of this report is structured as follows: a note about the technical implementation of IC4 within WW3 (Section 1.1), a description of all of the methods available and some idealized studies of attenuation (Section 2), and a case study evaluated against field data (Section 3).

## 1.1 A Note on Implementation

As with all source terms in WW3, IC4 needs to be declared in the switch file. In addition, the method is set by the integer value (1, 2, 3, 4, 5, or 6) for IC4METHOD namelist parameter in the ww3_grid.inp file. If an integer value is not declared or incorrectly entered, the method will default to a calculation equal to IC1 where the attenuation is a constant read in from $C_{ice,1}$. There are up to 8 (5 ice parameters + 3 mud parameters) available which are referred to as $C_{ice,1}$, $C_{ice,2}$, ..., $C_{ice,5}$, MUDD, MUDT, and MUDV. Whereas in IC1, $C_{ice,1}$ is the user determined attenuation coefficient, for methods 1, 2, 3, and 4, these parameters are constants of the equations. Additionally, for method 3 $C_{ice,1}$ is ice thickness. Method 5 uses the parameters to describe four different attenuation rates and the frequency bands they apply to. Method 6 makes use of the namelist to extend M5. To activate, set the appropriate logicals associated with each ice parameter and give an input file for parameters changing in space or declare the values for homogeneous field data.

In terms of the 3-character IDs for "Homogeneous field data" in ww3_shel.inp, these are, respectively, `IC1'`, `IC2'`, `IC3'`, `IC4'`, `IC5'`, `MDN'`, `MTH'`, and so this might look like:

```
 'IC1'          19680606  000000          5.0e-6
 'IC2'          19680606  000000          7.0e-6
 'IC3'          19680606  000000          15.0e-6
 'IC4'          19680606  000000          100.0e-6
 'IC5'          19680606  000000          0.10
 'MDN'          19680606  000000          0.12
 'MTH'          19680606  000000          0.16
```

In the above context, `IC1'` and `IC4'` refer to "ice coefficients 1 and 4", not be confused with IC1 and IC4 as used in the rest of this report, which refers to the notation in the mode code for $S_{ice}$ physics routine #1 and $S_{ice}$ physics routine #4. See the WW3 manual, associated regression tests, and documentation in the code for further details on the implementation.

## 1.2 Observation and Application of Attenuation

It has long been known that waves attenuate as they enter icy waters, and measurements have shown that attenuation is exponential over distance (Squire and Moore, 1980; Wadhams et al., 1988). According to Eq. 1 of Wadhams et al. (1988):

$$E_x(f) = E_0(f) \exp(-\alpha x)$$

Here $x$ is the distance between the open water spectrum $E_0(f)$ and the in-ice spectrum $E_x(f)$. With a known distance between measurement locations, Eq. 1 may inverted to give an estimate of attenuation coefficient $\alpha$,

$$\alpha = \frac{\ln\left(\frac{E_x(f)}{E_0(f)}\right)}{x}$$

This is the general method for attaining the attenuation coefficient from measurements. You may notice that $\alpha$ is a function of frequency, $f$ or $\sigma = 2\pi f$, but it is also common to show $\alpha$ as a function period, $T = 1/f$. Measurements have shown that ice preferentially damps high frequency waves and in this way ice acts as a low pass filter (Robin, 1963; Marko, 2003; Collins, 2015). IC4 can reproduce this preferential damping, as well as other more recent observations about frequency and wave height dependent attenuation (Kohout et al., 2014; Meylan et al., 2014).

An alternative notation for attenuation is $k_i$ which originates from a more general representation of attenuation starting from the complex dispersion relation. There is a straightforward relationship between $k_i$ and $\alpha$.

$$k_i = \frac{\alpha}{2}$$

WW3 is based on the action balance equation. Wave action is conserved as waves propagate in time and space. Sources and sinks balance the gain and loss of wave action. For waves propagating in icy water, a new sink is required, $S_{ice}$. To calculate $S_{ice}$, the attenuation coefficient is applied to the action balance equation using the group velocity:

$$C_g \equiv \frac{\partial \omega}{\partial k}$$

and

$$\frac{S_{ice}}{E} = -C_g \alpha = -2C_g k_i$$

Here $E$ is the spectral density. The methods in IC4 provide a number of choices, empirically and theoretically based, for the structure of $\alpha(f)$.

# 2 IC4 methods

## 2.1 Method 1: Exponential fit to Wadhams et al. (1988)

Here we give attenuation that is exponential as a function of period. The default values are based on measurements from Wadhams et al. (1988). Wadhams et al. (1988) described measurements, made by accelerometers placed in line with direction of wave propagation going into ice, over the course of a number of field experiments in the Greenland and Bering Seas. Attenuation coefficient values logged in table 2 of Wadhams et al. (1988) were manually digitized and a fit to the data was calculated.
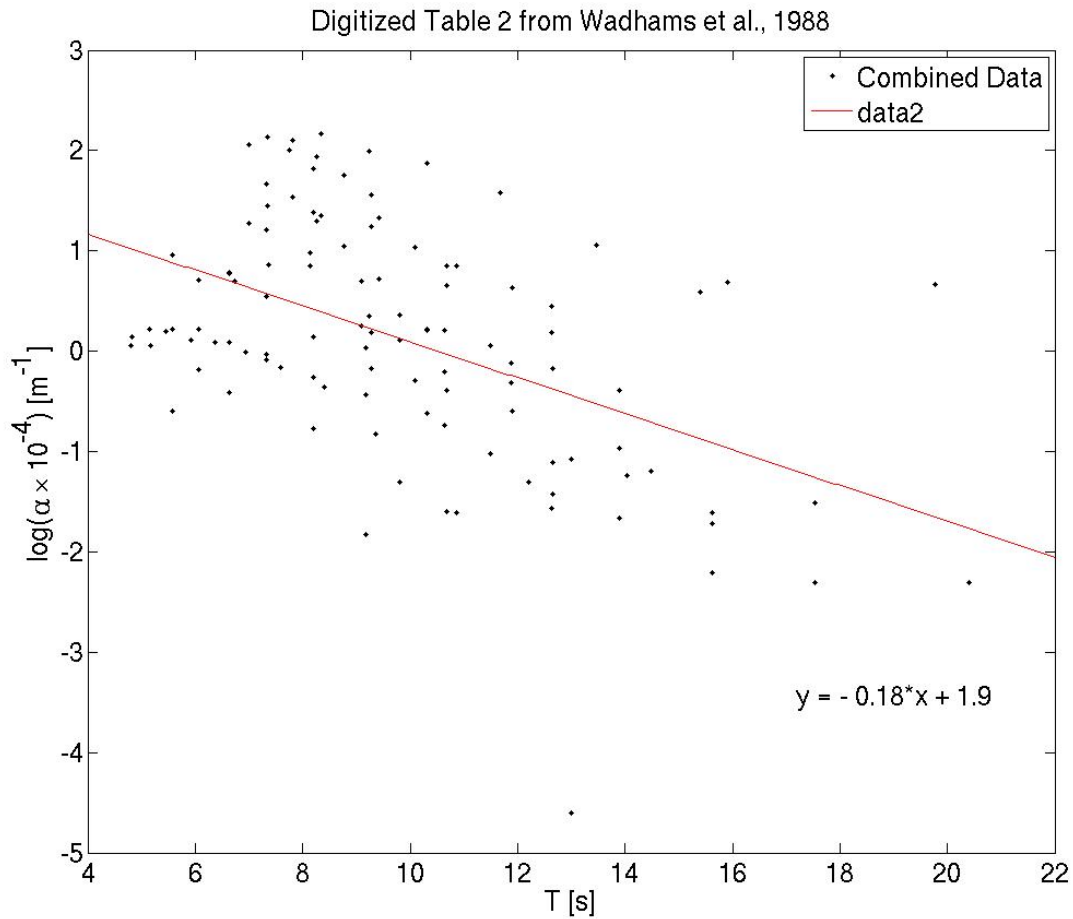
Figure 1 Data from Wadhams et al. (1988) plotted as natural log of attenuation coefficient as a function of period marked in black dots. The straight, red line is the least squares fit to the data, corresponding to Eq. 1 below.

Figure 1 shows the combined attenuation data of Wadhams et al. (1988) which was originally separated based varying ice conditions. For our purposes, we wanted a rough representation which might apply to all ice conditions and thus the data was combined. The red line shows the least squares fit to a linear equation in log space, which results in an exponential equation (Eq. 1). The fit qualitatively preserves the observation at the heart of the study: ice preferentially attenuates high frequency waves. Therefore, this is a parametrization of the well known low-pass filtering effect of ice. The equation has the following form:

$$\alpha = \exp\left[\frac{-2\pi C_{ice,1}}{\sigma} - C_{ice,2}\right] \tag{1}$$

The default values as determined from the of the data are [$C_{ice,1}$, $C_{ice,2}$] = [0.18, 7.3]. The user has the option to change these values and therefore represent any exponential function as a function of period.

## 2.2 Method 2: Polynomial fit of Meylan et al. (2014)

Here the user gives coefficents of $4^{th}$ degree polynomial, giving a flexible method for prescribed attenuation. The default values come from Meylan et al. (2014). Meylan et al. (2014) measured attenuation in the Antarctic through an ice field with buoys. They justify a polynomial fit to their data by noting that the low frequency attenuation appeared to be proportional to wavenumber, but with higher attenuation rates for high frequency waves requiring a second term with more strongly nonlinear dependence on frequency. Their Eq 3. is the following:

$$\alpha = C_{ice,1} + C_{ice,2} \left[\frac{\sigma}{2\pi}\right] + C_{ice,3} \left[\frac{\sigma}{2\pi}\right]^2 + C_{ice,4} \left[\frac{\sigma}{2\pi}\right]^3 + C_{ice,5} \left[\frac{\sigma}{2\pi}\right]^4$$

From Meylan et al. (2014), the default values for the coefficients are $[C_{ice,1...5}]$ = [0, 0, 2.12E-3, 0, 4.59E-2]. Non-default settings are allowed in WW3: in other words, the user is able to change all the coefficients of the polynomial and therefore shape of the attenuation function.

## 2.3 Method 3: Quadratic Fit to Kohout and Meylan (2008) given in Horvat and Tziperman (2015)

Horvat and Tziperman (2015) fit a quadratic equation to the attenuation coefficients calculated by the scattering model Kohout and Meylan (2008) as a function of period, $T$, and ice thickness, h. Attenuation increases as ice thickness and frequency increases, respectively. The ice thickness, which we write as $h$ in the following equation, is input by the user as the ice parameter $C_{ice,1}$.

$$\alpha(T, h) = \exp\left(-0.3203 + 2.058h + -0.9375T + -0.4269h^2 + 0.1566 * hT + 0.0006 * T^2\right)$$

Be advised, the equation itself was an extrapolation of the original range of $h$ used to calculate the attenuation coefficients in Kohout and Meylan (2008) which was between 0.5 and 3 m. See Horvat and Tziperman (2015) for more details.

## 2.4 Method 4: Eq.1 from Kohout et al. (2014)

Using the same Antarctic data as Meylan et al. (2014), Kohout et al. (2014) found that attenuation was a function of significant wave height. For this formulation, attenuation is constant across frequencies but increases as a linear function of $H_s$. This dependency is capped off for waves of 3 m and higher, thus:

$$\begin{cases} \dfrac{dH_s}{dx} = C_{ice,1}H_s & \text{for } H_s \leq 3 \\ \dfrac{dH_s}{dx} = C_{ice,2} & \text{for } H_s > 3 \end{cases}$$

The values given in Kohout et al. (2014) are $[C_{ice,1...2}]$ = [5.35x10$^{-6}$, 16.05x10$^{-6}$].

## 2.5 Method 5: Four Part Step Function

Method 5 gives attenuation as a step function in frequency space with four steps. $C_{ice,1...4}$ determine the values of attenuation at each step and the $C_{ice, 5...7}$ designate the end of the frequency range (in Hz) of the first 3 steps, respectively. An example, given in the source code, was determined by inverting the attenuation coefficient from observations from an AWAC mooring in the Beaufort Sea on Aug 27 - 30, 2012. The values for the parameters were given as follows $[C_{ice,1...7}]$ = $[5 \times 10^{-6}, 7 \times 10^{-6}, 15 \times 10^{-6}, 100 \times 10^{-6}, 0.10, 0.12, 0.16]$. In practice, WW3 only permits up to five non-uniform ice parameters, so $C_{ice,6}$ and $C_{ice,7}$ are input by the user by borrowing parameter space from two coefficients used for non-uniform viscous mud: MUDD and MUDT.

## 2.6 Method 6: Step Function via namelist

Method 6 is identical to Method 5, except that:
1. Parameters in Method 5 can be (optionally) non-uniform in space and time, and for Method 6, they are always uniform in space and time.
2. The procedure for inputting parameters is more convenient to the user in Method 6 (Fortran namelist).
3. Method 5 allows up to 4 steps, and Method 6 allows up to 10 steps.
4. Method 5 precludes simultaneous use of a viscous mud physics parameterization.

A specific example of IC4 Method 6 is discussed in Section 4.2.4, "$S_{ice}$ Parameterizations"

## 2.7 Attenuation

The difference between each of these methods can be visualized by plotting the attenuation coefficient with the default inputs.

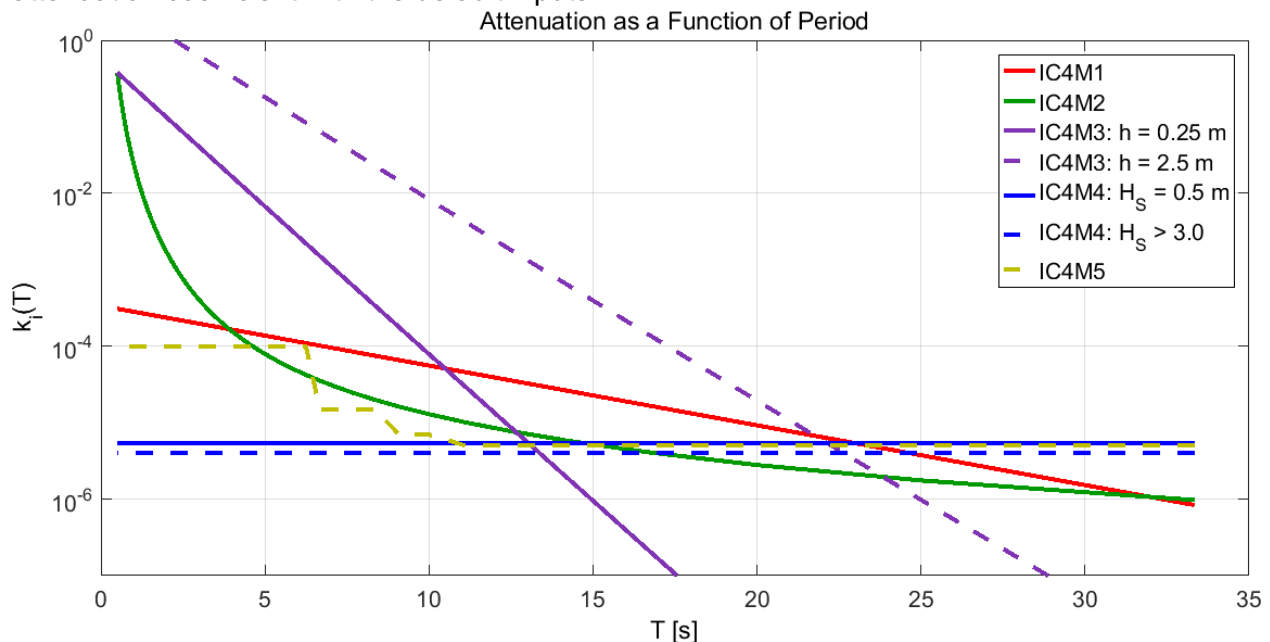

Attenuation as a Function of Period

Figure 2 The value of the attenuation coefficient is shown as a function of period for different methods in IC4. Method 1 is shown in red, method 2 in green, method 3 in solid purple for ice thickness of 0.25 m and dashed purple for ice thickness of 2.5 m, method 4 in solid blue for a significant wave height of 0.5 m and dashed blue for significant wave heights greater than 3.0 m, and method 5 in dashed gold with the values given in the example.
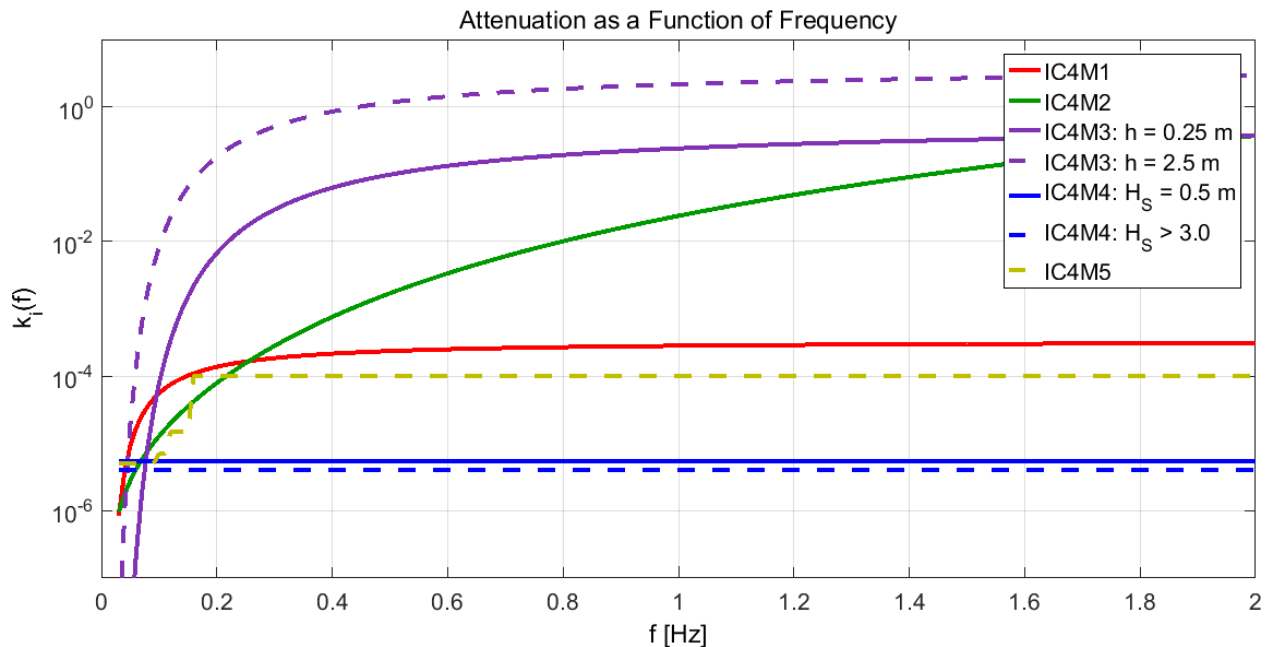


Figure 3 As in Figure 2, but horizontal axis is now frequency.

For each method, with the exception of M4, attenuation is function of frequency. As can be seen in Figure 2-3, the attenuation varies across several decades for the same period of frequency depending on the method. This variation reflects the variation found in measurements, and to no small degree, the variation of ice conditions encountered during the experiments. Though such variation from one case study to another is easily understood, applying this knowledge in operational forecasting remains a severe challenge, due to operational uncertainty of ice conditions, particularly in the Marginal Ice Zone (MIZ).

# 3 Regression Testing

WW3 is a community-developed model, and regression testing ("reg-tests") arose as an aid in maintaining functional model code as researchers simultaneously made changes and updates. There are four reg-tests associated with ice source terms: ww3_tic1.1, ww3_tic1.2, ww3_tic1.3, and ww3_tic2.1. Within ww3_tic1.1, various input files are maintained, including those for IC4: input_IC4. Within IC4 there are 5 subdirectories corresponding to each of the 5 methods: M1, M2, M3, M4, and M5. See the run_test script for instructions on running a reg-test.

For the following test, we modify reg-test ww3_tic1.1 to verify that our calculations are behaving as expected. Regression test ww3_tic1.1 is set up for one-dimensional wave

propagation through an ice layer. An active boundary supplies the wave field which propagates over space-time into the ice. The model runs for 12 hours, and by the end of the model run the wave height at each grid points is approximately steady state. The grid is 154 km of ice cover with 1 km resolution. We modify the default case of the incoming boundary condition from a monochromatic wave to a 4 m (significant wave height) JONSWAP wave spectrum. For M4, the ice thickness is set 0.25 m, the rest of the methods uses the default parameter inputs maintained in their respective input directories.
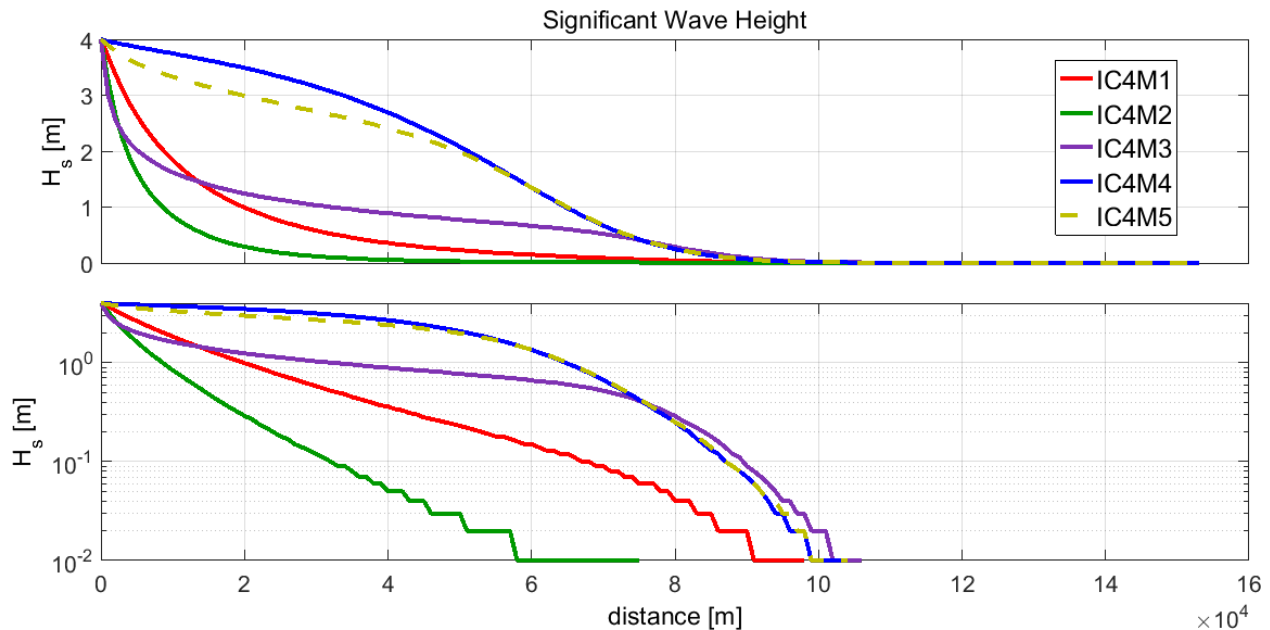


Figure 4 Significant wave height as a function of distance into the ice. Top plot y-axis is linear scale, bottom plot y-axis is on a log scale. The different methods, M1-5, are shown in red, green, purple, blue, and dashed gold, respectively.

Figure 4 shows significant wave height as a function of distance into the ice after 12 hours of propagation. While the significant wave height depends on distance into the ice, the smallest significant wave height consistently results from M2 with default settings.

While Figure 4 shows the attenuation of significant wave height, it is useful also to verify that attenuation is indeed applied as a function of frequency across the spectrum. To show this, we compare the 1D wave frequency spectra as result of the application of IC1 and IC4M1 at 5 and 10 km into the ice after 12 hours.
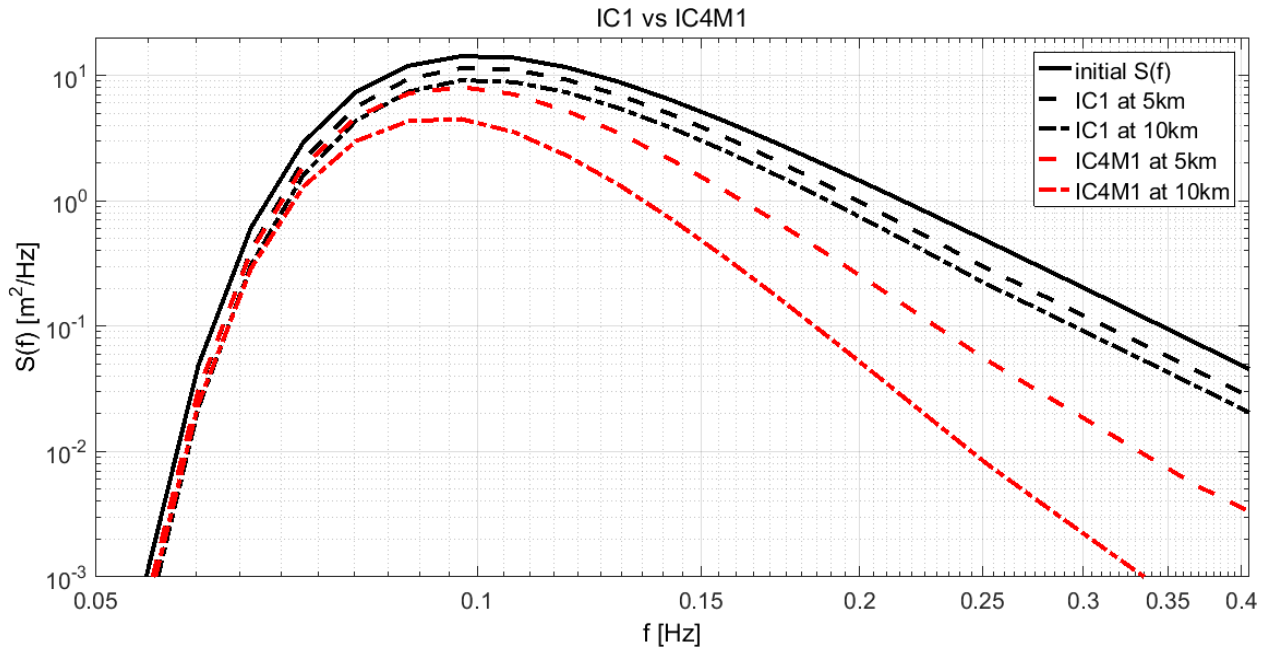
Figure 5 Change in spectra as a function of distance due to attenuation, based on regression test ww3_tic1.1 run with IC1 and 1C4 method 2. The black line is the initial spectrum input at the boundary. The solid (dashed) lines show the spectra 5 (10) km into the ice with IC1 shown in black and IC4 method 1 in a red. [NB: the wave spectrum *S(f)* is denoted as *E(f)* elsewhere in this report.]

Figure 5 shows the wave spectrum at the active boundary, 5 km into the ice, and 10 km into the ice. The active boundary condition is identical between runs. The attenuation resulting from IC1 is constant as a function of frequency and thus the shape of the spectrum is maintained. For IC4M1, the attenuation is a function of frequency so that the high frequency face is steeper and the peak frequency has shifted slightly to lower frequencies. For most of the methods which preferentially attenuate high frequency waves, the change in spectral shape will be qualitatively similar: steepening high frequency face and a shift of the peak to lower frequencies.

Quantitatively, the shape of the spectrum is a result of attenuation as a function of frequency (see Figure 3) and will be different for each method. For example, the identical regression test run with IC4M2 yields Figure 6.

Figure 6 Change in spectra as a function of distance due to attenuation, based on regression test ww3_tic1.1 run with IC4 method 2. The black line is the initial spectrum input at the boundary. The spectra at 1, 2, 5, 10, and 15 km into the ice are shown in green solid, dashed, dotted, dash-dot, and marked with circles, respectively. [NB: the wave spectrum *S(f)* is denoted as *E(f)* elsewhere in this report.]

Figure 6 shows IC4 method 2 with the boundary condition in blue and 4 locations in the ice: 1, 2, 5, and 10 km. Notice the steepening of the high frequency face and the shift of the peak to slightly lower frequencies.

Next, we compare effect of attenuation on wave spectra methods for M1-5. In Figure 7, spectra are shown at 5 and 10 km.
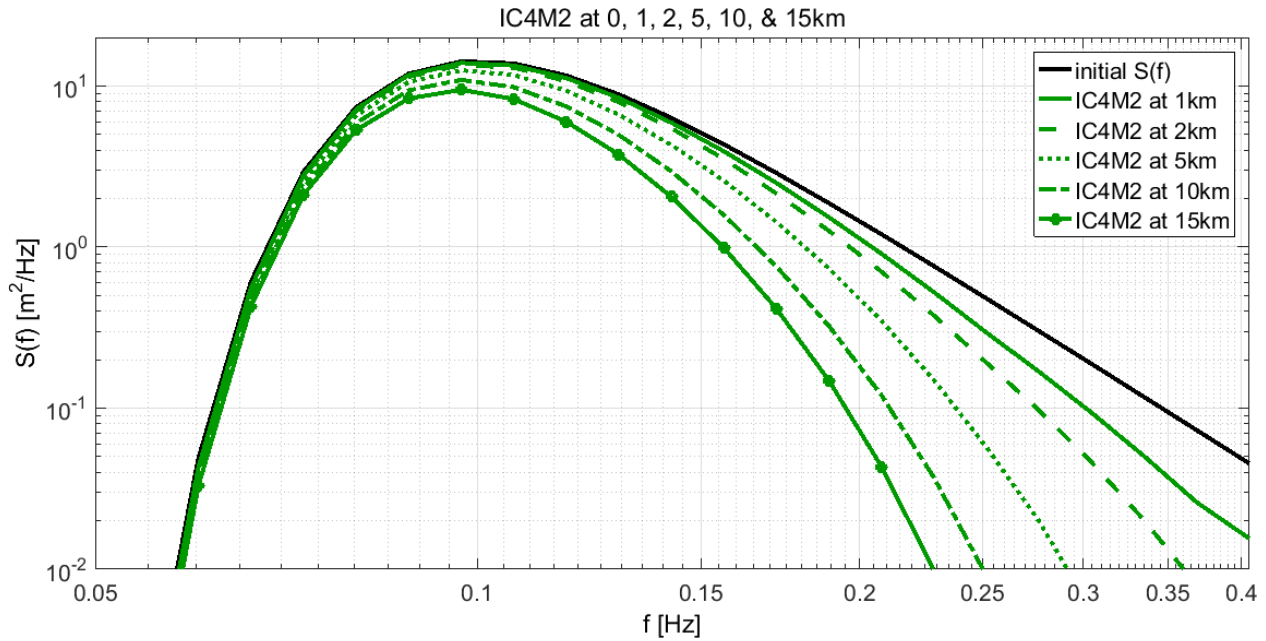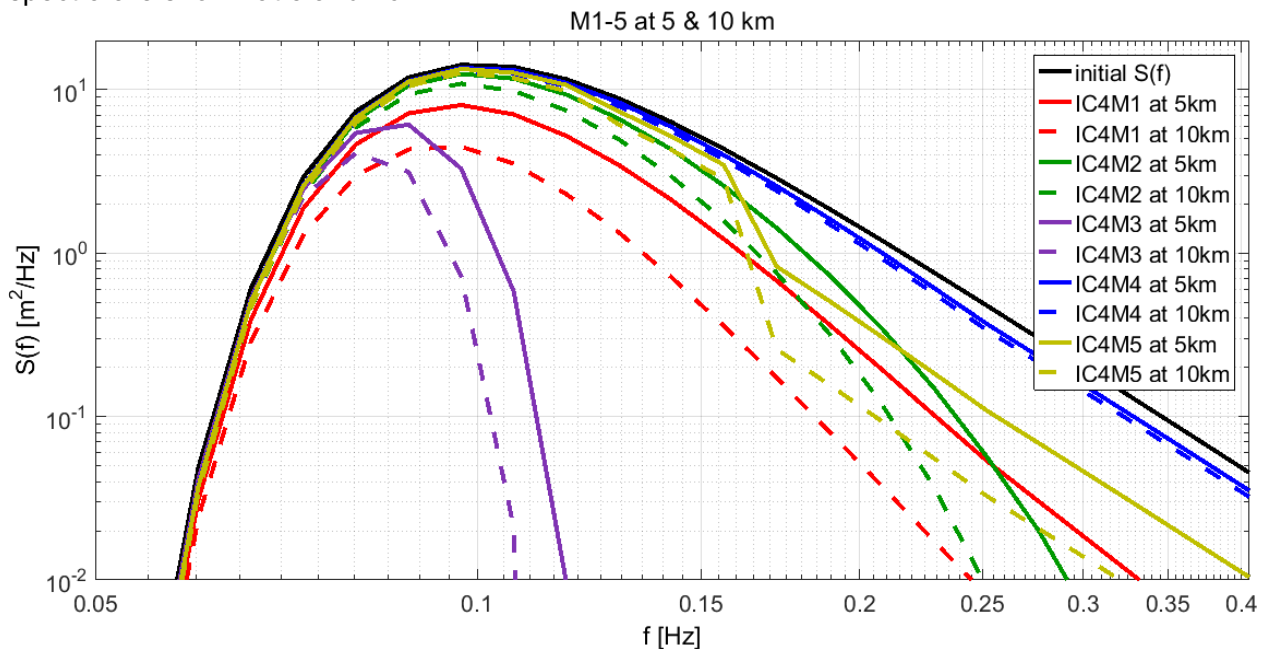


Figure 7 Change in spectra as a function of distance due to attenuation, based on regression test ww3_tic1.1 run with IC4 methods 1-5. The black line is the initial spectrum input at the boundary. The spectra 5 and 10 km are shown with

solid and dashed lines. The methods are represented in the different colors: red, green, purple, blue, and gold for methods 1, 2, 3, 4, and 5, respectively. [NB: the wave spectrum $S(f)$ is denoted as $E(f)$ elsewhere in this report.]

# 4 Case Study

## 4.1 Arctic Sea State Experiment

In the autumn 2015, the Office of Naval Research (ONR) supported a field experiment in the Beaufort and Chukchi Seas, and neighboring Arctic Ocean, as part of the Departmental Research Initiative (DRI) "Sea State and Boundary Layer Physics of the Emerging Arctic Ocean" (Thomson et al., 2013). Some of the analysis herein (Figures 9 and 12-14) pertain to a 3-day period from Oct. 11-13, 2015 known as wave array 3 (WA3), while the rest pertain to the wave measurements taken during the entire field experiment. During WA3 a number wave sensors were deployed from the R/V Sikuliaq which included University of Washington SWIFT buoys (Thomson et al., 2012), Cambridge University directional buoys, and a buoy developed at New Zealand's National Institute for Water and Atmospheric Research buoy (similar to Kohout, 2015). The buoys were deployed in an array approximately in the wave direction.

The waves were created by the interaction of a high and two low pressure systems, the strongest of which was situated over the Gulf of Alaska. The winds were aligned along a thin stretch of open water in the Beaufort Sea with northern Alaska making up a southern boundary and sea ice episodically advancing from the central Arctic being a permeable northern boundary. The maximum winds over the fetch were ~ 23 ms-1 resulting in wind sea with 4 – 5 m significant wave height at the peak of the storm in a direction from the southeast.

## 4.2 Model Setup

### 4.2.1 Grids

The model is run in a nested fashion, with two irregular grids. The outer grid has 10 km resolution and the inner grid has 5 km resolution. The outer grid is a polar stereographic grid covering half the Arctic, including portions north of eastern Siberia, Alaska, and most of Canada (cyan region in Figure 8). Swell energy from outside this grid is excluded, as it is insignificant within the study area. The inner WW3 grid fully encloses the study area, and is also shown in Figure 8, as a black rectangle. This grid has a central meridian at 156.5W (near Barrow, Alaska), and grid lines were constructed by tracing great circles west and east from the central meridian, starting from points at 5 km intervals on the meridian, with grid points at 5 km intervals along the great circles.
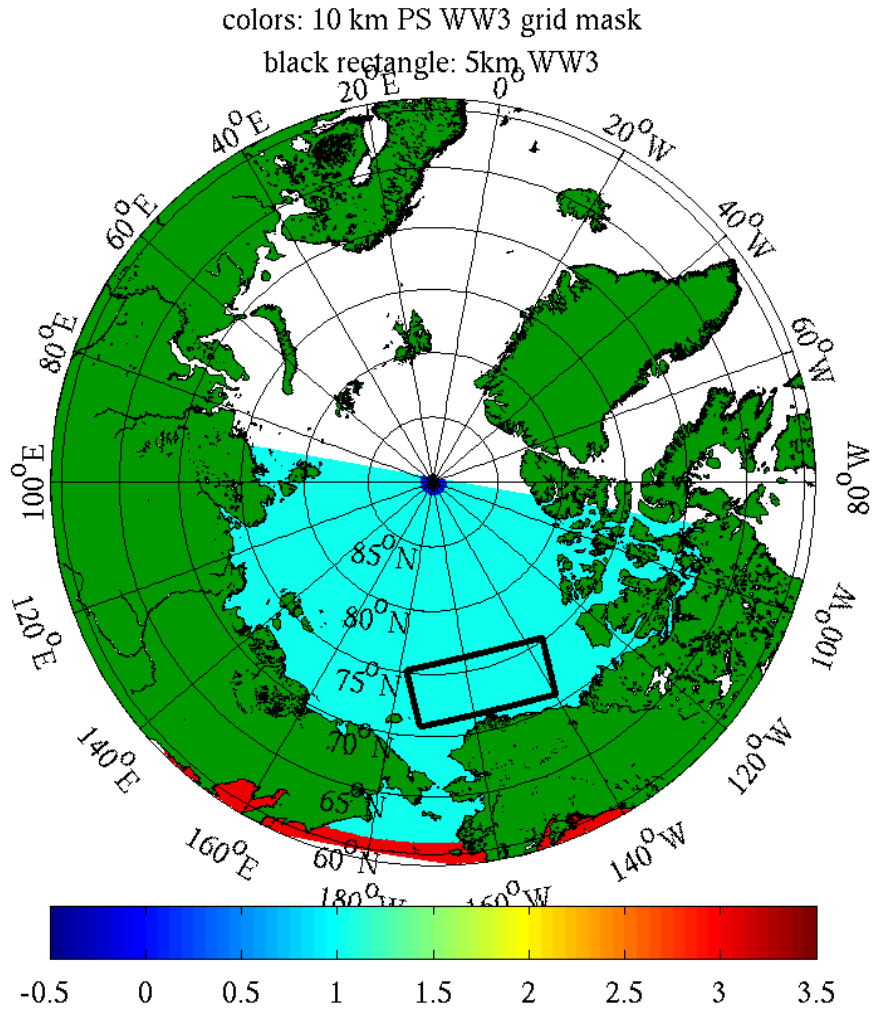
Figure 8 Wave model grids. Cyan region indicates active grid points in outer WW3 grid. Red region indicates excluded (masked) areas. Black rectangle is the bounding box for the inner WW3 grid.

All WW3 results presented below are from the inner WW3 grid.

## 4.2.2 Inputs

The model uses wind forcing from the Navy's global meteorological model, NAVGEM (Hogan et al. 2014), at 0.5 degree resolution.

Ice concentration for the outer grid is from AMSR2 (Advanced Microwave Scanning Radiometer 2), onboard the GCOM-W (Global Change Observation Mission) satellite operated by JAXA (the national space agency of Japan). This is at 3.125 km resolution, with one field per day, and is remapped to the WW3 resolution (10 km). The timestamp on each field is shifted forward to 1200 UTC, to center it temporally. This dataset comes from the University of Hamburg: Beitsch et al. (2013, 2014).

Ice concentration for the inner (5 km) WW3 grid is also taken from AMSR2, but at higher temporal resolution. AMSR2 swath data was provided by Dr. Li Li (NRL Code 7223) on a 10 km grid. These swaths do not all pass over the study area, and we only include swaths which cover a large majority (90%) of a rectangle tightly enclosing the cruise track (this track is shown in Figure 9). Prior swaths are used to fill in gaps. The swath-selection criterion results in a forcing which is irregular in time: there are 157 unique fields provided to the model over 35 days, so the average interval between ice concentration update in the model is 5.3 hours.

It may seem like a contradiction that the AMSR2 product with lower geographic resolution (10 km) is used for the higher resolution WW3 grid (5 km), while the higher resolution AMSR2 product (3.125 km) is used for the lower resolution WW3 grid (10 km). Our reasoning is as follows: We selected the 10 km AMSR2 product for the inner grid as it better captures the fast changes observed in the ice during the field experiment. We selected the 3.125 km AMSR2 product for the outer grid because direct use of swath data is not possible for a large region, due to the limits of the swath width.

## 4.2.3 Settings and Initialization

Settings used for all grids are as follows:
- 36 directional bins
- 30 frequency bins, from 0.045 to 0.7138 Hz
- overall time step is 900 s
- Ardhuin et al. (2010) physics (denoted "ST4").
- ST4 physics has a parameter, $\beta_{max}$ ("BETAMAX" in the WW3 code), intended to be adjusted to accommodate gross wind bias. (Altering this parameter is, in practice, similar to a "blunt tool" adjustment of the wind speeds.) In these simulations, we used $\beta_{max} = 1.1$. This is a relatively low value, appropriate to the positive bias of the NAVGEM wind forcing. It is judged appropriate by comparison of WW3 total energy to data measured by SWIFT buoy S11 below: this is our "open water reference" buoy.

Settings for the outer grid are as follows:
- Run time is 2015-09-20 1200 UTC to 2015-11-10 0000 UTC (cold start)
- propagation time step is 450 s

Settings for the inner grid are as follows:
- Run time is 2015-10-01 1500 UTC to 2015-11-10 0000 UTC (hot start, see below)
- propagation time step is 225 s

The inner grid is hot-started on 2015-10-01 1500 UTC a prior simulation with the same grid, using the 24-hourly AMSR2. That simulation is cold-started on 2015-09-20 1200 UTC (same as the outer grid). Here, we use the term "cold start" to indicate that there is a period of spin-up with invalid output, though the model was not actually started from

rest. We judge that for this relatively small basin, the 10-day spin-up time is much more than is actually required (in other words, conservative).

## 4.2.4 $S_{ice}$ Parameterizations

Results from six simulations with the inner grid are used below. The six are as follows:
- a model run with $k_i$=0 (and so $S_{ice}$=0). Note that this does not mean that there are no ice effects. Ice concentration still affects the model insofar as the open water fraction is used to scale the wind input and breaking terms (see Rogers et al. 2016 or WW3DG 2016).
- IC4M1
- IC4M2
- IC4M3 with ice thickness ($h_{ice}$) = 25 cm
- IC4M4
- IC4M6 with a step function based on the "P/FR-H" profiles (red lines) in Figure 9 of Rogers et al. (2016)*. The "P/FR-H" denotes that it is based on pancakes and frazil ice mixture, in the more highly dissipative grouping, which corresponds to thicker frazil in the buoy ice photos (see that paper for full explanation). IC4M6 with these settings is denoted as "IC4M6H" herein.

*For readers who wish to use IC4M6H in WW3, the namelist setting is:

```
&SIC4  IC4METHOD = 6,
    IC4FC =      0.10   , 0.15 , 0.20 , 0.25 , 0.30 ,
                 0.35   , 0.40 , 99.0 , 0.00 , 0.00
    IC4KI =      2.94e-06, 4.27e-06, 7.95e-06, 2.95e-05, 1.12e-04,
                 2.74e-04, 4.95e-04, 8.94e-04, 0.00      , 0.00
                 /
```

# 4.3 Results

We use four parameters for wave model performance. All use some form of spectral moments: $m_n = \int_{f1}^{f2} E(f) f^n df$, where $f$ is frequency and $E(f)$ is the non-directional (1d) spectrum.

1. $H_{m0}$, significant wave height, proportional to the square root of total energy : $H_{m0} = 4\sqrt{m_0}$
2. "Tm01E4", or $T_{m,01,E4}$ , the mean period $T_{m,01}$ of $E(f)^4$ , a parameter for dominant wave period, $T_{m,01,E4} = \frac{\int_{f1}^{f2} E(f)^4 df}{\int_{f1}^{f2} E(f)^4 f df}$. This has two positive characteristics: it is smooth (since it is based on integration) and it is close to the peak period (by using the fourth power on $E(f)$).
3. "Tmm10", or $T_{m,-1,0}$ : another parameter for dominant wave period, $T_{m,-1,0} = m_{-1}/m_0$.
4. $m_4$, the fourth moment of the wave spectrum, proportional to mean square slope. This metric is sensitive to high frequency energy level, and so responds strongly to any damping of high frequencies by ice cover.

In all cases, the frequency bounds on the integration, $f_1$ and $f_2$, are set such that they are consistent between model and observations. This is ensured by outputting spectral density $E(f)$ from WW3 and performing the integration as a post-processing step.

For ground truth we use buoy data collected during the field experiment. This comes from two basic types: moored buoys and drifting buoys.

**Moored buoys**

There were two moored subsurface "AWAC" (Nortek Acoustic Wave And Current) buoys collecting data in the region during the Sea State cruise, marked with diamonds in Figure 9. The southwest location was at a "one-off" mooring site (159.01W, 72.64N), and the AWAC was deployed and recovered by the Sikuliaq during the cruise (Thomson 2015). This is denoted as "AWACSS" here. The northeast mooring was at a recurring site (150W, 75N), "Beaufort Gyre A", denoted as "AWACBGA" here. Both AWACs are owned and operated by the Applied Physics Laboratory, U. Washington (APL/UW). AWACBGA was deployed by the Canadian Coast Guard icebreaker Louis S. St.-Laurent contemporary with the Sea State cruise (October 7 2015). This site is one of three Beaufort Gyre moorings maintained by the Woods Hole Oceanographic Institution.
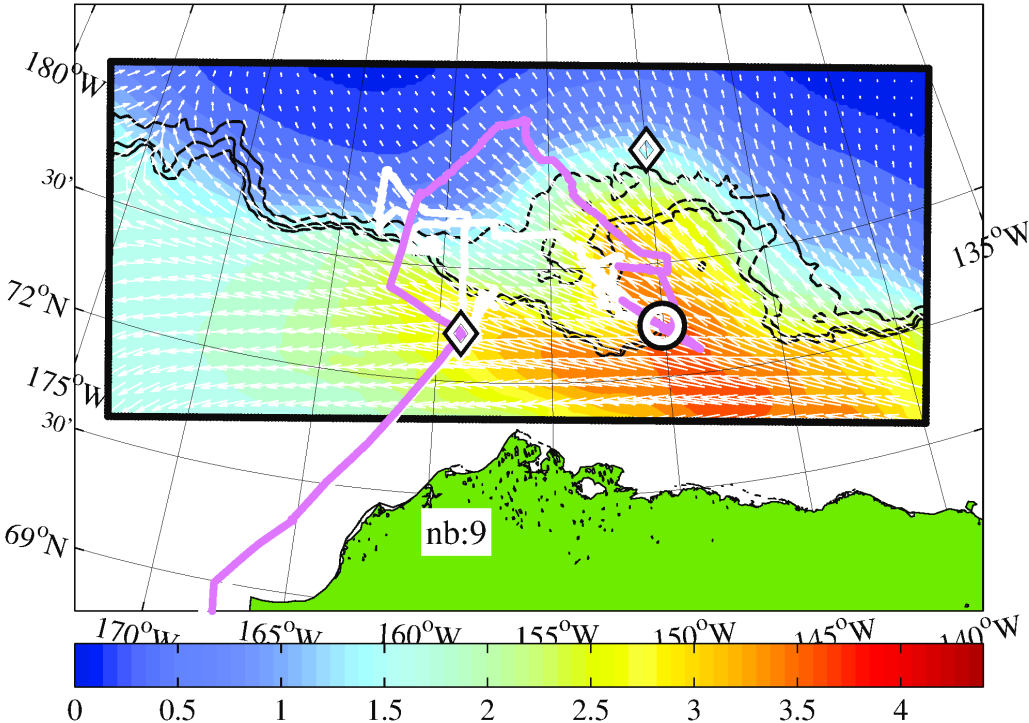


Figure 9 Example result from inner WW3 grid for 1200 UTC 12 Oct. 2015. Colors indicate significant wave height in meters. Arrows indicate mean wave direction. Contours indicate ice concentration (25%, 50%, 75%). "nb:9" indicates that 9 drifting buoys were deployed at this time. Diamonds indicate active, moored AWACs. Circle indicates location of R/V Sikuliaq. Thick magenta and white lines indicate path of R/V Sikuliaq (past and future ship position, respectively).

Extracting *E(f)* output from WW3 is straightforward in the case of moored data: the "point output" feature of WW3 is used.

**Drifting buoys**

Three types of drifting wave buoys were deployed during the R/V Sikuliaq cruise:

1. "SWIFT" buoys, engineered and operated by Dr. Jim Thomson and the APL/UW engineering team (see e.g. Thomson 2012). The data were processed by Ms. Madison Smith (APL/UW).
2. "British" buoys, designed and operated by Dr. Martin Doble (Polar Scientific) as part of a project led by Prof. Peter Wadhams (Cambridge University) with U.S. Office of Naval Research (ONR) funding.
3. "NIWA" buoys, designed and operated by Dr. Alison Kohout of the National Institute of Water and Atmospheric Research (New Zealand).

All of the scientists mentioned above participated in the cruise and planned the wave experiments.

In case of (1) and (2), data are available from several wave experiments (denoted as "wave arrays") during the cruise. In case of (3), all data used here is from Wave Array #3 (WA3) October 10-14 2015. More info on the wave arrays and buoy deployments can be found in Thomson (2015) and Wadhams and Thomson (2015). Additional information about WA3 data can be found in the WW3 modeling study Rogers et al. (2016), where data from (1) and (2) were utilized. In the present study, spectra were provided such that each represents a 30-minute interval. SWIFT buoys are centered at 15 and 45 minutes after the hour, while British buoys are centered at 0 and 30 minutes after the hour.

Extracting *E(f)* output from WW3 is not simple in the case of drifting buoys. The "track output" feature of WW3 is used. Latitude/longitude/time triplets are provided to WW3, which stores output not at these points, but at the bounding computational grid points. As a post-processing step, *E(f)* is integrated into the three wave parameters ($H_{m0}$, $T_{m,01,E4}$, $m_4$) and these parameters are bi-linearly interpolated to the buoy locations.

Figure 9 shows WW3 grid 2 example results from IC4M4 during WA3, 2015 October 12 1200 UTC.

Figure 10 shows wave height and Figure 11 shows dominant wave period time series, comparing AWACSS observations to results from the six $S_{ice}$ parameterizations. AWACSS is in open water during the entire duration, but results are sensitive to the $S_{ice}$ parameterization for much of the time series, especially October 18-25. This sensitivity occurs when wave energy travels through the ice before reaching the mooring. IC4M2 and IC4M3 over-predict dissipation Oct 20-23, implying that these are more appropriate for thicker and/or more rigid ice conditions. IC4M1 is less dissipative, and so predicts wave height fairly well during that period, though wave period is very low, suggesting a that the spectral distribution of dissipation is not appropriate to these ice conditions.

IC4M4 and IC4M6H have the best bias characteristics for the largest fraction of the time series.

The $m_4$ comparison is excluded from the AWACSS time series due to concerns about the quality of the AWACSS dataset at higher frequencies.
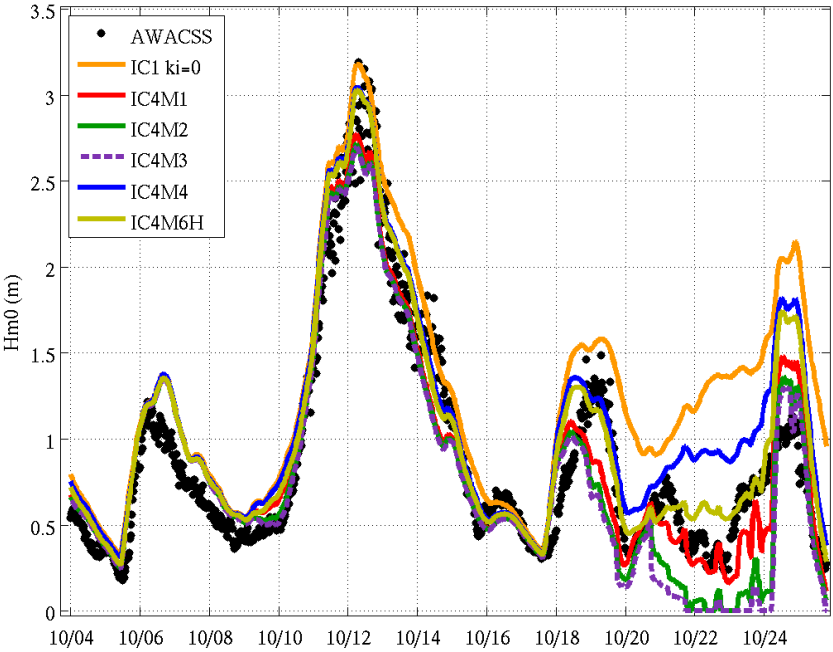


Figure 10 Time series of significant wave height $H_{m0}$ for AWACSS vs. 6 models.
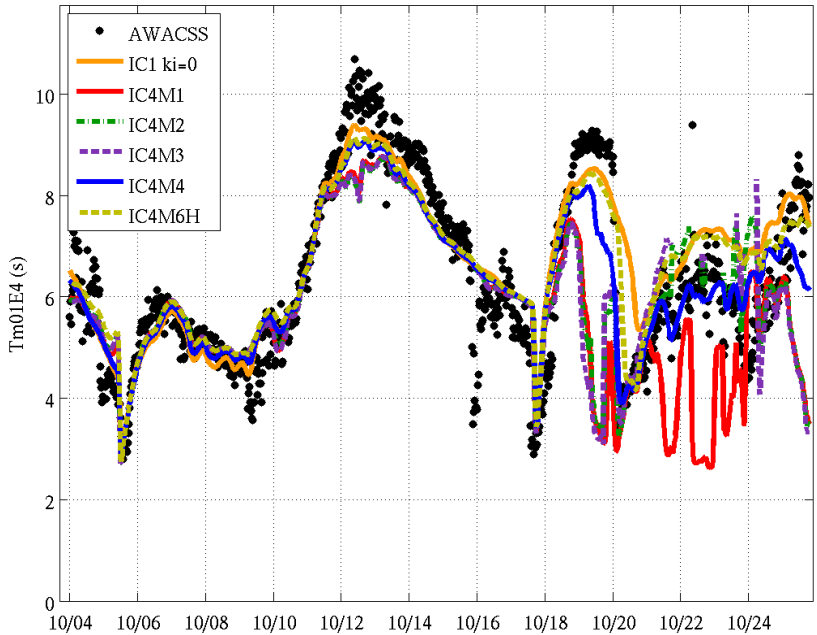


Figure 11 Time series of dominant wave period $T_{m,01,E4}$ for AWACSS vs. 6 models.

17

WA3 is studied for the same six models in Figure 12 to Figure 14. For sake of brevity, we only look at $H_{m0}$ this time.

SWIFT 11, denoted "S11" here, is used to evaluate the "incident wave conditions", since this buoy is believed to have been in open water for all of the wave experiment. As expected, the outcome is only weakly sensitive to the ice parameterization (important to note: the vertical axis in the S11 figure does not extend to zero). The small sensitivity which does exist is associated with wave energy which must pass through ice to the east: though the predominant wave direction is "from southeast", directional spreading means that some energy is "from east". The S11 comparison is a useful check on the open water generation physics of the model, and the meteorological forcing. The comparison indicates that some temporal variability in the observed $H_{m0}$ (3.20 to 3.95 m in the latter 80% of the time series) is not captured by the model (3.55 to 3.80 in the same period), which implies that the meteorological forcing is too smooth (a common problem), and that, at any given time, up to 40 cm of error may be associated with the wind forcing, and systematic error is +12 to +21 cm (positive bias). This bias is not ideal, but is tolerable, taken in context of the 300 to 380 cm wave heights.

SWIFT 14, denoted "S14" here, was in a mixture of pancakes and frazil ice for most of the experiment. This may be broadly characterized as "fluidized" ice cover, insofar as it moves as a fluid within the scale of a model grid cell. IC4M2 and IC4M3 are clearly unsuitable for this type of ice cover, and IC4M1 is only slightly better. IC4M4 underpredicts dissipation, which IC4M6 performs best, which is not surprising given that it is based on inversion for this wave experiment. Overprediction of wave energy by both IC4M4 and IC4M6H in the latter half of this time series is explained as follows: S14 was in a narrow feature of thick fluidized ice during this period, while the model treats that area as open water, as the feature is too small to show up in the AMSR2 forcing. This problem will be detailed in a subsequent NRL report which focus on WW3 forcing (i.e. input fields) during this cruise.

For AWACBGA, the ice cover was most likely continuous ice which is sufficiently flexible to permit wave propagation without systematic ice break-up. (If fracturing did occur, it is not apparent in the Sentinel-1 Synthetic Aperture Radar imagery, not shown.) Unsurprisingly, the IC4M6H model, which is based on fluidized ice, underpredicts the dissipation in this type of ice cover. A less obvious outcome (from the author's point of view) is that the models M1, M2, and M3 still severely overpredict the dissipation. This is presumably associated with the ice cover here being thin relative to the ice cover in those prior studies.
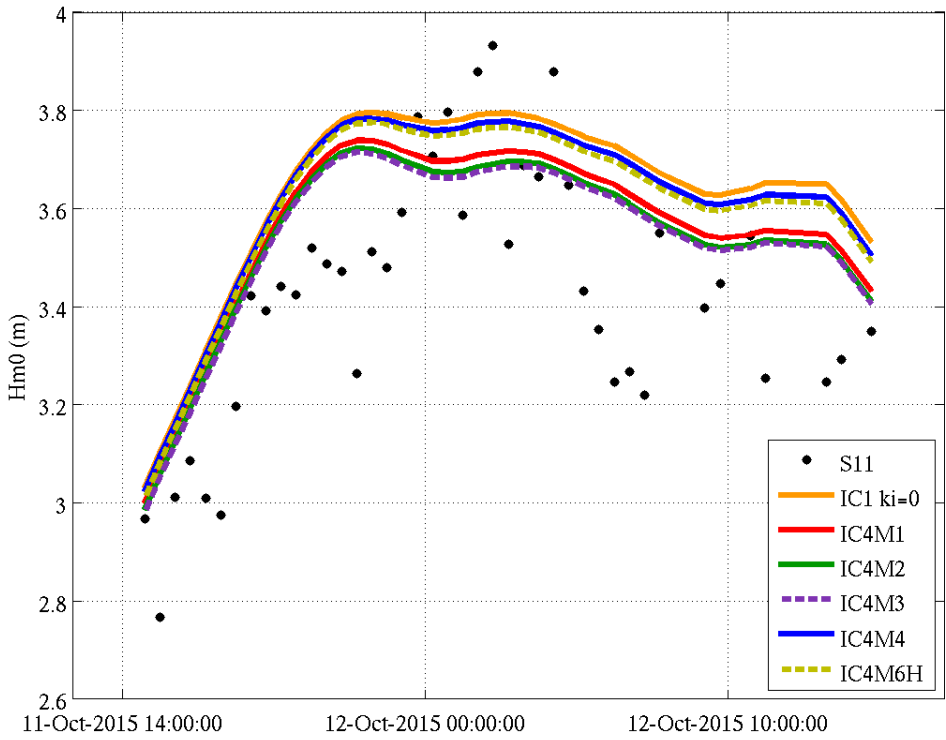
Figure 12 Time series of significant wave height $H_{m0}$ for SWIFT-11 (incident condition, open water) vs. six models. (NB: The minimum of the vertical axis is not zero.)
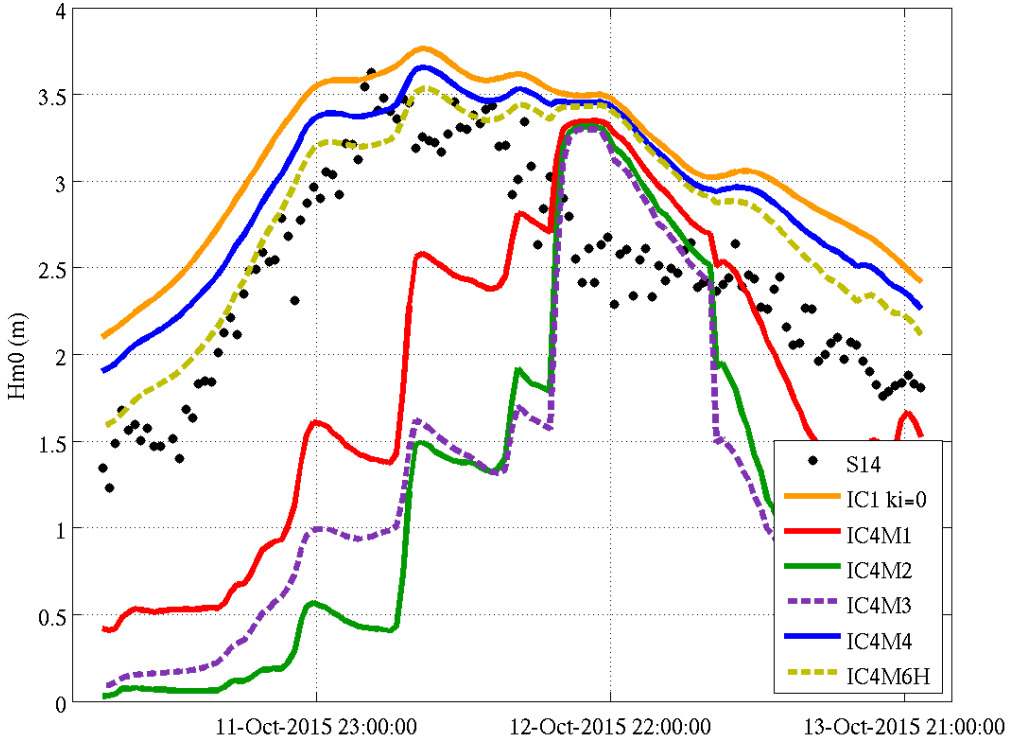


Figure 13 Time series of significant wave height $H_{m0}$ for SWIFT-14 (in-ice condition: pancakes and frazil) vs. six models.
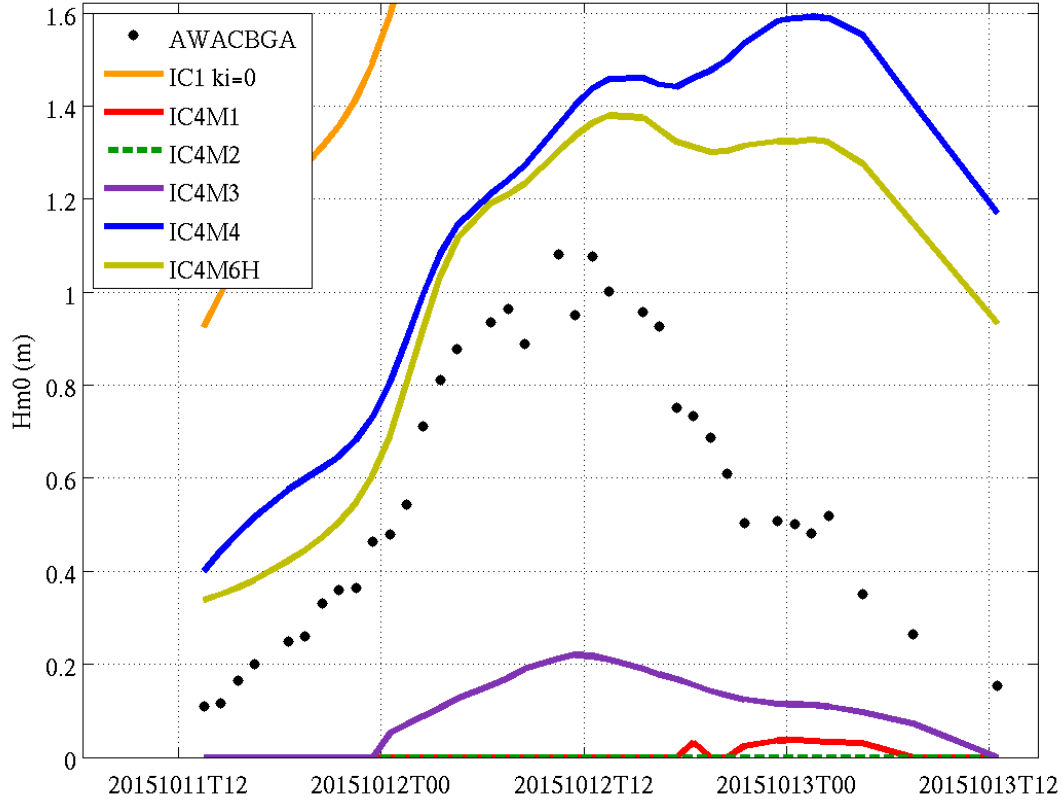
Figure 14 Time series of significant wave height $H_{m0}$ for AWACBGA (in-ice condition: sheet ice) vs. six models.

Statistics were calculated for all six models, for AWAC and drifting buoys. For sake of brevity, we show only the IC4M4 and IC4M6H models here.

Table 1 Statistics using drifting buoys as ground truth. All wave experiments.

| parameter | model | n | CC | SI | RMSE | bias | nbias |
|-----------|-------|-----|------|------|--------|--------|--------|
| $H_{m0}$ | IC4M4 | 2590 | 0.96 | 0.30 | 0.41 | 0.18 | 0.14 |
| $H_{m0}$ | IC4M6 | 2590 | 0.96 | 0.30 | 0.37 | 0.02 | 0.02 |
| $T_{mm10}$ | IC4M4 | 2054 | 0.81 | 0.15 | 1.20 | -0.71 | -0.11 |
| $T_{mm10}$ | IC4M6 | 2054 | 0.85 | 0.13 | 0.90 | -0.08 | -0.01 |
| $m_4$ | IC4M4 | 2054 | 0.78 | 0.78 | 2.9e-04 | 2.2e-04 | 0.86 |
| $m_4$ | IC4M6 | 2054 | 0.82 | 0.70 | 1.8e-04 | 3.4e-05 | 0.13 |

Units for $H_{m0}$, $T_{mm10}$, $m_4$ in RMSE and bias are m, s, and $m^2/s^4$, respectively. "n" is number of co-locations, "CC" is correlation coefficient, "SI" is scatter index, "RMSE" is root-mean-square error, bias is mean error, and "nbias" is normalized bias. Customary definitions are used for each, see e.g. Rogers and van Vledder (2013).

In these comparisons, the much larger positive normalized bias of the IC4M4 parameterization for $m_4$ parameter, relative to that of the IC4M6H parameterization, is highlighting something that is already known: to predict spectral shape in the ice with any accuracy, frequency-varying parameterization for $k_i$ must be used. With IC4M6H, compared to the drifting buoys, the modeled $m_4$ is reasonably accurate in the mean sense, though scatter is high for $m_4$ in both models.

Table 2 Statistics using AWACs as ground truth.

| platform | parameter | model | n | CC | SI | RMSE | bias |
|---|---|---|---|---|---|---|---|
| AWACBGA | Hm0 | IC4M4 | 36 | 0.60 | 0.57 | 0.64 | 0.55 |
| AWACBGA | Hm0 | IC4M6 | 36 | 0.73 | 0.46 | 0.49 | 0.42 |
| AWACSS | Hm0 | IC4M4 | 1040 | 0.94 | 0.24 | 0.29 | 0.20 |
| AWACSS | Hm0 | IC4M6 | 1040 | 0.96 | 0.21 | 0.22 | 0.12 |

Finally, we present the time series of these three wave parameters for the field experiment as a whole (Figure 15). Though this presentation does not permit one-to-one comparison for individual buoys, it provides a general picture for variety of wave conditions from one wave experiment to another, and a visual representation of the time-varying mean error of either model.
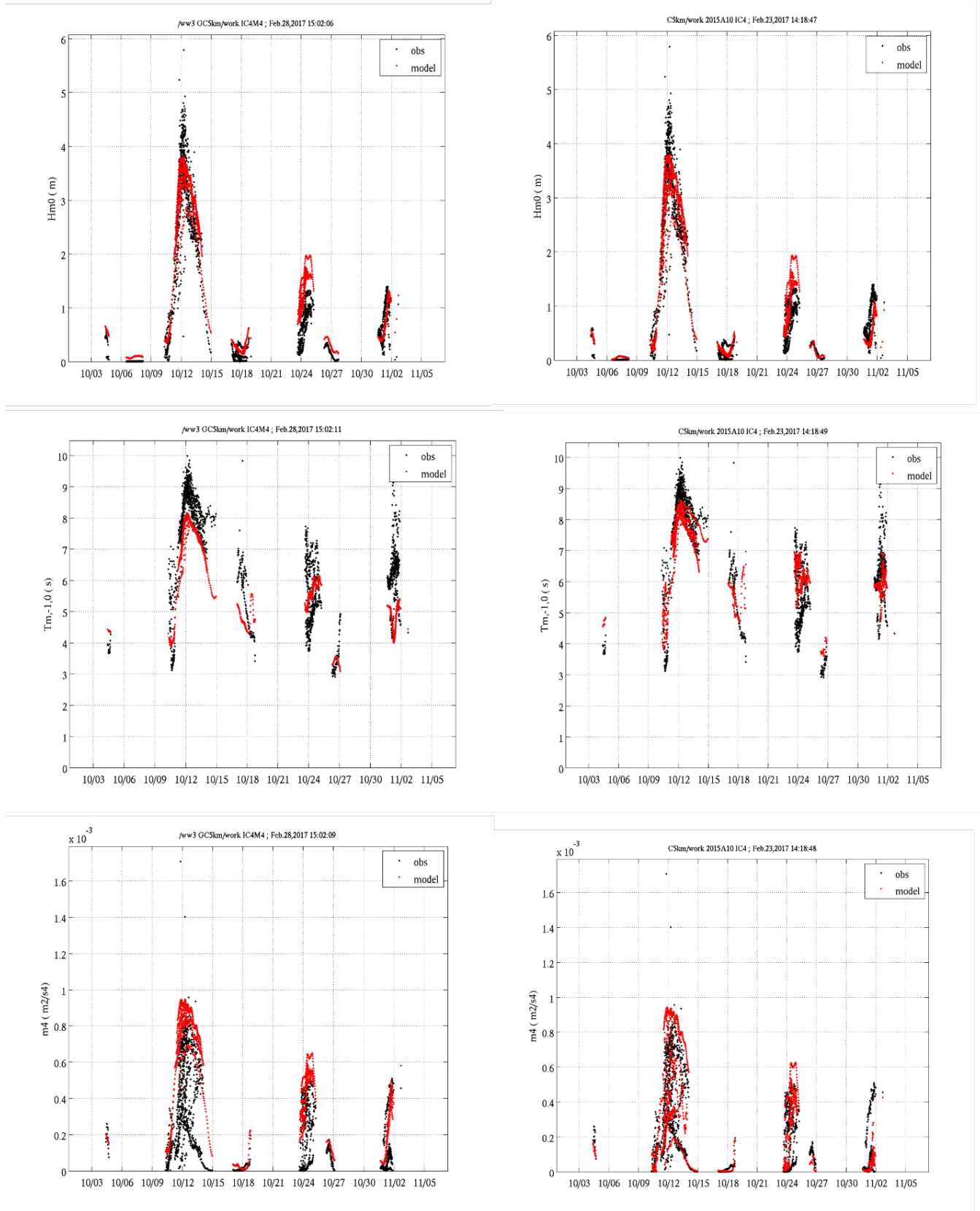
Figure 15 Time series plots for model vs. drifting buoys. Left: IC4M4 model. Right: IC4M6H model. Upper: $H_{m0}$; Center: $T_{m-1,0}$ ; Lower: $m_4$.

22

# 5 Acknowledgements

# 6 References

Beitsch, A., L. Kaleschke, S. Kern, and X. Tian-Kunze (2013), AMSR2 ASI 3.125 km Sea Ice Concentration Data, V0.1, Institute of Oceanography, University of Hamburg, Germany, digital media. (ftp-projects.zmaw.de/seaice/)

Beitsch, A.; Kaleschke, L.; Kern, S. Investigating High-Resolution AMSR2 Sea Ice Concentrations during the February 2013 Fracture Event in the Beaufort Sea (2014), Remote Sens., 6, 3841-3856.

Collins III, C. O., W. E. Rogers, A. Marchenko, and A. V. Babanin (2015), In situ measurements of an energetic wave event in the Arctic marginal ice zone. *Geophysical Research Letters*, *42*(6), 1863-1870.

Collins III, C. O., W. E. Rogers, and A. Marchenko (2016), On Wave-Ice Interaction in the Arctic Marginal Ice Zone: Dispersion, Attenuation, and Ice Response. NRL/MR/7320--16-9676

Collins III, C. O., W. E. Rogers, and B. Lund (2017), On Dispersion of Wind Generated Ocean Surface Waves in Ice Covered Seas. Ocean Dynamics, 67, 263–280.

Hogan, T., and 16 Coauthors (2014), The Navy Global Environmental Model, Oceanography, 27(3), 116-125.

Horvat, C. and E. Tziperman (2015), A prognostic model of sea-ice floe size and thickness distribution. The Cryosphere, 9, 2,119–2,134.

Kohout, Alison L., et al. "A device for measuring wave-induced motion of ice floes in the Antarctic marginal ice zone." Annals of Glaciology 56.69 (2015), 415-424.

Kohout, A. L. and M. H. Meylan (2008), An elastic plate model for wave attenuation and ice floe breaking in the marginal ice zone. J. Geophys. Res., 113, C09016.

Kohout, A., M. Williams, S. Dean and M. Meylan (2014), Storm-induced sea-ice breakup and the implications for ice extent. Nature, 509, 604–607.

Marko, J.R. (2003), Observations and analyses of an intense waves-in-ice event in the Sea of Okhotsk. *Journal of Geophysical Research: Oceans (1978–2012)*, *108*(C9).

Meylan, M., L. Bennets and A. Kohout (2014), In situ measurements and analysis of ocean waves in the antarctic marginal ice zone. Geophys. Res. Lett., 41, 5,046–5,051.

Mosig, J. E., F. Montiel, and V. A. Squire (2015), Comparison of viscoelastic-type models for ocean wave attenuation in ice-covered seas. *Journal of Geophysical Research: Oceans*, *120*(9), pp.6072-6090.

Robin, G.D.Q. (1963), Wave propagation through fields of pack ice. *Philosophical Transactions of the Royal Society of London A: Mathematical, Physical and Engineering Sciences*, *255*(1057), pp.313-339.

Rogers, W. E., and M. D. Orzech (2013), *Implementation and testing of ice and mud source functions in WAVEWATCH III. NRL Memorandum Report*. NRL/MR/7320–13-9462, 31 pp.(http://www7320. nrlssc. navy. mil/pubs. php)

Rogers, W.E., and G.Ph Van Vledder (2013), Frequency width in predictions of windsea spectra and the role of the nonlinear solver, Ocean Modeling, 70, 52-61.

Rogers, W. E., and S. Zieger (2014), *New Wave-Ice Interaction Physics in WAVEWATCH III*. 22nd IAHR International Symposium on Ice. Singapore, Malaysia. August 11 to 15, 2014

Rogers, W. E., and S. Zieger (2014), $S_{ice}$: Damping by sea ice, in User Manual and System Documentation of WAVEWATCH III[®] Version 4.18b, edited by H. L. Tolman, pp. 60 –61, NOAA/NWS, College Park, MD Tech. Note, MMAB Contribution 31

Rogers, W.E., J. Thomson, H.H. Shen M.J. Doble, P. Wadhams and S. Cheng (2016), Dissipation of wind waves by pancake and frazil ice in the autumn Beaufort Sea, Journal of Geophysical Research: Oceans vol 121 7991-8007 doi:10.1002/2016JC012251

Squire, V.A. (2007), Of ocean waves and sea-ice revisited. *Cold Regions Science and Technology*, *49*(2), pp.110-133.

Thomson, J. (2012), Wave breaking dissipation observed with "SWIFT" drifters. Journal of Atmospheric and Oceanic Technology, 29(12), pp.1866-1882.

Thomson, J., Squire, V., Ackley, S., Rogers, E., Babanin, A., Guest, P., Maksym, T., Wadhams, P., Stammerjohn, S., Fairall, C., Persson, O., Doble, M., Graber, H., Shen, H., Gemmrich, J., Lehner, S., Holt, B., Williams, T., Meylan, M., Bidlot, J. (2013), "Science plan: Sea state and boundary layer physics of the emerging Arctic Ocean" Technical Report 1306, Applied Physics Laboratory, University of Washington.

Thomson, J. (2015), ONR Sea State DRI Cruise Report: R/V Sikuliaq, Fall 2015 (SKQ201512S), 45 pp., University of Washington, Seattle, Wash. [Available at http://www.apl.washington.edu/project/project.php?id5arctic_sea_state, last accessed 9 Aug. 2016.]

Tolman, H. and the WAVEWATCH III ® Development Group (2014), User Manual and System Documentation of WAVEWATCH III ® Version 4.18b, edited by H. L. Tolman, pp. 282, NOAA/NWS, College Park, MD Tech. Note, MMAB Contribution 31.

The WAVEWATCH III® Development Group (WW3DG) (2016), User manual and system documentation of WAVEWATCH III® version 5.16. Tech. Note 329, NOAA/NWS/NCEP/MMAB, College Park, MD, USA, 326 pp. + Appendices.

Wadhams, P., (2000), *Ice in the Ocean*. CRC Press.

Wadhams, P., and J. Thomson (2015), The Arctic Ocean cruise of R/V Sikuliaq 2015, An investigation of waves and the advancing ice edge, Il Polo, LXX-4, 9–38.

Wadhams, P., V. A. Squire, D. J. Goodman, A. M. Cowan, and S. C. Moore (1988), The attenuation rates of ocean waves in the marginal ice zone. Journal of Geophysical Research: Oceans (1978–2012) 93, no. C6: 6799-6818.